Time-resolved Ultraviolet Spectroscopy of the M-dwarf GJ 876 Exoplanetary System[*]

Kevin France[1], Jeffrey L. Linsky[2], Feng Tian[3,4], Cynthia S. Froning[1], Aki Roberge[5]

ABSTRACT

Extrasolar planets orbiting M-stars may represent our best chance to discover habitable worlds in the coming decade. The ultraviolet spectrum incident upon both Earth-like and Jovian planets is critically important for proper modeling of their atmospheric heating and chemistry. In order to provide more realistic inputs for atmospheric models of planets orbiting low-mass stars, we present new near- and far-ultraviolet (NUV and FUV) spectroscopy of the M-dwarf exoplanet host GJ 876 (M4V). Using the COS and STIS spectrographs aboard the *Hubble Space Telescope*, we have measured the $1150 - 3140$ Å spectrum of GJ 876. We have reconstructed the stellar H I Lyα emission line profile, and find that the integrated Lyα flux is roughly equal to the rest of the integrated flux ($1150 - 1210$ Å $+ 1220 - 3140$ Å) in the entire ultraviolet bandpass ($F(Ly\alpha)/F(FUV+NUV) \approx 0.7$). This ratio is $\sim 2500\times$ greater than the solar value. We describe the ultraviolet line spectrum and report surprisingly strong fluorescent emission from hot H_2 ($T(H_2) > 2000$ K). We show the light-curve of a chromospheric + transition region flare observed in several far-UV emission lines, with flare/quiescent flux ratios ≥ 10. The strong FUV radiation field of an M-star (and specifically Lyα) is important for determining the abundance of O_2 – and the formation of biomarkers – in the lower atmospheres of Earth-like planets in the habitable zones of low-mass stars.

[1]Center for Astrophysics and Space Astronomy, University of Colorado, 389 UCB, Boulder, CO 80309; kevin.france@colorado.edu

[2]JILA, University of Colorado and NIST, 440 UCB, Boulder, CO 80309

[3]Current Address: Center for Earth System Sciences, Tsinghua University, Beijing, China 100084

[4]Laboratory for Atmospheric and Space Physics, University of Colorado, Boulder, CO 80309

[5]Exoplanets and Stellar Astrophysics Laboratory, NASA Goddard Space Flight Center, Greenbelt, MD 20771

Subject headings: planetary systems — stars: individual (GJ 876) — ultraviolet: stars — stars: activity — stars: low-mass

1. Introduction

The advent of large radial velocity surveys and the *Kepler* mission (Udry et al. 2007; Borucki et al. 2011) have revealed planets with masses several times that of Earth in orbits that may permit the existence of liquid surface water (Kasting et al. 1993). Perhaps the most favorable objects for follow-up studies in the next decade are planets in the habitable zone (HZ) around low-mass stars, dwarfs of spectral type M0V and later (also referred to as M-dwarfs or dM stars). These planets have received considerable theoretical attention, and a consensus is emerging that neither synchronous rotation nor close proximity to the host star rules out the possibility of biological development on these worlds (Joshi 2003; Segura et al. 2005; Wordsworth et al. 2010).

The heating and chemistry of an Earth-like atmosphere depends strongly on the characteristics of the host star, both spectrally and temporally. The photospheric ultraviolet (UV) continuum of M-stars is very small relative to solar-type stars due to their lower effective temperature; bright chromospheric and transition region emission lines dominate the UV spectrum of M-dwarfs, containing a much larger fraction of the stellar luminosity than for solar-type stars. These differences influence the atmospheric temperature profile and the production of potential biomarkers (e.g. ozone, O_3; Segura et al. 2003; Segura et al. 2005). H_2O, CH_4, and CO_2 are highly sensitive to far-UV radiation, with photo-absorption cross-sections that overlap with H I Lyα, the strongest emission feature in the UV spectrum of an M-star. M-stars are known to display frequent and intense flare activity (Hawley et al. 1996; West et al. 2004; Welsh et al. 2007), and the combination of UV-photon and proton bombardment from a large flare may produce $\gtrsim 90\%$ O_3 depletions in an Earth-like atmosphere (Segura et al. 2010). Despite the importance of understanding these host M-stars, their actual spectral and temporal behavior is not well known outside of a few active flare stars (Linsky & Wood 1994; Pagano et al. 2000; Hawley et al. 2003; Osten et al. 2005).

GJ 876 is an M4V star ($M_* = 0.33\ M_\odot$) hosting a multi-planet system (Delfosse et al. 1998; Marcy et al. 1998, 2001; Rivera et al. 2005, 2010; Correia et al. 2010). The four planets have masses ranging from super-Jovian to super-Earth ($M_b = 2.64\ M_{Jup}$, $a_b = 0.21$ AU; $M_c = 0.83 - 0.86\ M_{Jup}$, $a_c = 0.13$ AU; $M_d \approx 6\ M_\oplus$, $a_d = 0.02$ AU; $M_e = 12\ M_\oplus$, $a_e = 0.33$ AU), with GJ 876b orbiting near the center of the HZ. Conditions favorable for the sustained presence of liquid surface water might therefore exist on any satellites of GJ 876b. There is no present evidence for a bright remnant debris disk around GJ 876 (Shankland et al. 2008),

and taken together with the slow stellar rotation ($40 \leq P_* \lesssim 97$ days; Rivera et al. 2005, 2010), GJ 876 is estimated to have an age between $0.1 - 5$ Gyr (Correia et al. 2010). On the basis of its Hα absorption spectrum, GJ 876 is often considered to be an inactive M-dwarf. However, GJ 876 has a measureable level of coronal emission in soft X-rays ($L_X \sim 3 \times 10^{26}$ erg s^{-1} in the $0.2 - 2.0$ keV band; Poppenhaeger et al. 2010). Walkowicz et al. (2008) have further challenged the assumed link between optical activity indicators and UV flux, using low-resolution HST-ACS prism observations to demonstrate that GJ 876 has levels of chromospheric near-UV (NUV) flux comparable to the well-studied active M-dwarf AD Leo.

Other than the low-resolution spectra presented by Walkowicz et al. (2008), there are very few NUV observations of GJ 876, and none that clearly detect emission from the star at far-UV wavelengths (FUV; $1150 < \lambda < 2000$ Å). As current M-dwarf models do not properly account for chromospheric and transition region emission, the lack of observational basis means that a crucial input to atmospheric models of planets orbiting low-mass stars is missing. The situation is sufficiently unclear that atmospheric modelers have taken widely varying approaches to estimating the UV radiation field incident upon the HZ of M-dwarfs, from assuming the UV spectrum of a young flare star (AD Leo; Wordsworth et al. 2010) to assuming an effective UV flux of zero (Kaltenegger et al. 2011). As suggested by the latter authors, constraints from direct observation are required. In order to address this situation, we have begun to acquire MUSCLES (Measurements of the Ultraviolet Spectral Characteristics of Low-mass Exoplanetary Systems). In this Letter, we present our first results from MUSCLES; NUV and FUV spectra of GJ 876 obtained with the *Hubble Space Telescope*-Cosmic Origins Spectrograph (COS) and Space Telescope Imaging Spectrograph (STIS).

2. *HST* Observations

GJ 876 was observed with COS and STIS on 05 January 2012 and 12 November 2011, respectively (*HST* Program ID 12464). Multiple central wavelengths and focal-plane offset (FP-POSs) settings with the COS G130M and G160M modes (G130M: FP-POS = 4, λ1300 and λ1327; G160M: FP-POS = 2, λ1589 and λ1623) were used to create a continuous FUV spectrum from $1143 - 1798$ Å. These modes provide a point-source resolution of $\Delta v \approx 17$ km s^{-1} with 7 pixels per resolution element (Osterman et al. 2011). We smoothed the data to the 17 km s^{-1} instrumental resolution for analysis. The total exposure times in the G130M and G160M modes are 2017s and 2779s, respectively. We aligned and coadded the one-dimensional spectra produced by the COS calibration pipeline, CALCOS, using the custom software procedure described in Danforth et al. (2010).

Because COS is a slitless spectrograph, observations at H I Lyα are heavily contaminated by geocoronal emission. We therefore observed the stellar Lyα profile with STIS, using the G140M/cenwave 1222 mode ($\Delta v \approx 30$ km s^{-1}) mode through the $52'' \times 0.1''$ slit for a total of 1138s. Using the G230L mode on STIS, we also acquired the 1800 – 3140 Å spectrum of GJ 876 at $\Delta v \lesssim 400$ km s^{-1}.

3. Spectrally and Temporally Resolved Ultraviolet Spectra of GJ 876

3.1. The UV Spectrum of GJ 876

In Figure 1, we display the full 1150 – 3140 Å UV spectrum of GJ 876 (*red*). We observe emission from atomic and ionic species tracing a range of formation temperatures, including Lyα, C II, Al II ($T \sim 1 - 3 \times 10^4$ K); C III, Si III, Si IV, He II ($T \sim 6 - 8 \times 10^4$ K); C IV, N V, and O V ($T \sim 1.0 - 1.6 \times 10^5$ K). These emission lines clearly indicate that there is an active chromosphere and transition region on this star. As suggested by Walkowicz et al. (2008), GJ 876 is *not* an inactive star when observed in the UV. The STIS G230L observations show emission lines from Mg II and Fe II as well as a weak NUV continuum at $\lambda > 2200$ Å. In Figure 1, we plot the flux observed at the orbit of GJ 876b, roughly centered in the HZ of GJ 876 ($F_{HZ} = F_{obs} \times (d/a_b)^2$; $a_b = 0.21$ AU). The HZ spectrum of GJ 876 is compared with the Solar spectrum (*black*; Woods et al. 2009), evaluated at 1 AU. The GJ 876 data have been convolved with a 2 Å FWHM Gaussian kernel for comparison with the Solar data. Table 1 presents the band- and line-integrated HZ fluxes for several key regions/species.

3.2. Reconstruction of the H I Lyα Emission Line Profile

In order to produce an accurate estimate of the Lyα flux incident on the planets in the GJ 876 system, the Lyα profile observed by STIS must be corrected for attenuation by interstellar hydrogen and deuterium (e.g., Ehrenreich et al. 2011). In order to do this, we approximate the intrinsic Lyα emission line as a two-component Gaussian (as suggested for transition region emission lines from late-type stars by Wood et al. 1997) and create a simultaneous least-squares fit to the stellar emission and interstellar absorption components. The Lyα emission components are characterized by an amplitude, FWHM, and velocity centroid ($v_{emis}^{narrow,broad}$). Interstellar absorption is parameterized by the column density of neutral hydrogen (N(HI)), Doppler b parameter, D/H ratio, and the velocity of the interstellar absorbers (v_{ISM}). For this work, we assumed a fixed D/H ratio (D/H $= 1.5 \times 10^{-5}$; Linsky et

al. 1995; 2006).

A two-component fit with FWHMs = 133 and 303 km s^{-1}, and an interstellar atomic hydrogen absorber characterized by $\log_{10}(N(\text{H I})) = 18.06$ and $b = 8.0$ km s^{-1}, is able to produce an adequate fit ($\chi_\nu^2 = 1.73$) to the observations. The best model has $v_{emis}^{narrow} = +2.4$ km s^{-1}, $v_{emis}^{broad} = -8.0$ km s^{-1}, and $v_{ISM} = -3.0$ km s^{-1}; the Lyα emission is somewhat blueshifted relative to the +8.7 km s^{-1} radial velocity of the star. The ISM velocity from our best-fit model is consistent with the expected Local Interstellar Cloud velocity towards GJ 876 ($v_{LIC} = -3.56$ km s^{-1}; Redfield & Linsky 2008), supporting our Lyα reconstruction analysis. A single Gaussian Lyα emission line is unable to reproduce the observed profile ($\chi_\nu^2 > 6$), confirming our choice of a two-component emission model. The reconstructed stellar Lyα profile is shown in Figure 2. Integrated over the model profile, the total intrinsic Lyα flux is 4.38×10^{-13} erg cm^{-2} s^{-1}. The uncertainty on the integrated intrinsic flux is $\approx 5 - 10$ %, while the uncertainty on any individual fit parameter is most likely ≈ 20 %. We note that the correction for interstellar scattering does not take into account higher order opacity sources such as the stellar wind and heliosphere, which are not expected to significantly affect our results (Wood et al. 2005).

3.3. H$_2$ Fluorescence

A surprising result from the COS G160M observations is the detection of relatively strong molecular hydrogen fluorescence. We clearly detect six H$_2$ emission lines pumped by Lyα through the $(1-2)$ R(6) $\lambda 1215.73$ Å and $(1-2)$ P(5) $\lambda 1216.07$ Å transitions. The lines pumped through $(1-2)$ R(6) are: [$(1-7)$R(6) $\lambda 1500.24$ Å and $(1-7)$P(8) λ 1524.65 Å]. The lines pumped through $(1-2)$ P(5) are: [$(1-6)$R(3) $\lambda 1431.01$ Å, $(1-6)$P(5) λ 1446.12 Å,$(1-7)$R(3) $\lambda 1489.57$ Å, and $(1-7)$P(5) λ 1504.76 Å]. The Lyα-pumping mechanism requires a significant population of molecules in the $v = 2$ level of the ground electronic state, typically implying rotational temperatures of $T(\text{H}_2) > 2000$K (see Herczeg et al. 2004 and France et al. 2010a). The relative H$_2$/atomic line ratios are large compared with other M-stars (AD Leo, Proxima Cen, EV Lac, and AU Mic). Since the S/N of the individual H$_2$ lines is relatively low, we coadded the six cleanly detected lines (there were several other marginal detections). We fit the normalized line profile, incorporating the COS line-spread function (LSF; Figure 3). The line has a narrow, main component that is unresolved and at the radial velocity of the star (FWHM$_{H2}$ = 16.1 km s^{-1}; v_{H2} = +9 km s^{-1}). There is a second, marginally detected, broader component offset by -26 km s^{-1}. We present a discussion of the origin of the H$_2$ emission lines in §4.2.

3.4. FUV Flare

During the COS G130M observations of GJ 876, we observed a flare in several lines formed in the active upper atmosphere of the star, characterized by analyzing the emission line count rates as a function of time. The light curves were extracted from the calibrated three-dimensional data by exploiting the time-tag capability of the COS microchannel plate detector (France et al. 2010a). We extract a $[\lambda_i, y_i, t_i]$ photon list (where λ is the wavelength of the photon, y is the cross-dispersion location, and t is the photon arrival time) from each exposure i and coadd these to create a master $[\lambda, y, t]$ photon list. The total number of counts in a $[\Delta\lambda, \Delta y]$ box is integrated over a timestep Δt. The instrumental background level is integrated over the same wavelength interval as the emission lines, but offset below the active science region in the cross-dispersion direction. Figure 4 shows the count rates of C II $\lambda\lambda 1334,1335$, N V $\lambda\lambda,1239,1243$, Si III $\lambda 1206$, and the detector background, evaluated in $\Delta t = 40$s timesteps. The count rate in the emission lines at exposure times $T_{exp} > 4800$s is decaying from the flare maximum. The peak of the flare most likely occurred while the target was occulted by the Earth (the break in the observations between $T_{exp} \approx 1300 - 4800$ s), which prevents us from measuring the actual peak or the full decay time of the flare. However, the *observed* flare maximum is approximately $10\times$ the quiescent level, with an exponential decay time scale ~ 400s, implying a peak flare/quiescent FUV flux ratio of ≥ 10.

4. Discussion

4.1. The Importance of Lyα for Atmospheric Chemistry

Figure 1 and Table 1 show that the FUV/NUV ratio is much larger for M-dwarfs than for solar-type stars, and that the intrinsic Lyα flux dominates the HZ UV spectrum of GJ 876. Comparing the intrinsic Lyα flux to the rest of the FUV ($1150 - 1210 + 1220 - 1790$Å), we see that the Ly$\alpha$/(FUV) ratio is $\sim 8\times$ the solar value. The reconstructed Lyα emission line has roughly the same integrated flux as the rest of the UV spectrum ($1150 - 3140$ Å) combined. This is striking when compared to the relative contribution of Lyα to the total UV luminosity (Lyα/(FUV+NUV)) from the Sun. GJ 876 displays a Lyα/(FUV+NUV) ratio $\sim 2500\times$ larger than the solar value.

Because most of the UV luminosity from M-dwarfs is emitted in emission lines, molecular species in the atmospheres of orbiting planets will be "selectively pumped"; only species that spectrally coincide with stellar UV emission lines will be subject to large energy input from the host star. In order to estimate of the impact of Lyα irradiation, we computed the

total flux absorbed by several important atmospheric constituents, $F_{\lambda,abs}(X) = F_{FUV}(\text{GJ } 876) \times (1 - e^{-\tau_\lambda(X)})$, where $\langle \tau_\lambda(X) \rangle$ is calculated from published photoabsorption cross-sections for $X = CO_2$ (Yoshino et al. 1996), H_2O (Mota et al. 2005), or CH_4 (Lee et al. 2001). We find that Lyα photons account for $> 40\%$ of the energy absorbed by CO_2 and $> 85\%$ of the energy absorbed by H_2O and CH_4. Other chromospheric and transition region emission lines contribute only a few percent to the energy absorbed by H_2O and CH_4. C II, Si IV, and C IV each contribute $\sim 10\%$ to the FUV stellar flux absorbed by CO_2. While we are not presenting a rigorous treatment of the radiative transfer of Lyα photons incident on a planetary atmosphere (this will be done in future modeling work), this rough calculation highlights the importance of Lyα emission to the total energy budget available to drive atmospheric chemistry on these worlds.

Strong FUV flux should be included in models of terrestrial planets in the HZ of so-called "inactive" M-dwarf host stars. Stellar FUV flux will drive CO_2 photolysis, leading to an enhancement of atmospheric O_2 (and O_3), although the exact enhancement factor must be determined. Segura et al. (2007) showed that O_2 and O_3 column densities are enhanced by a factor of ~ 3 in CO_2-rich atmospheres when the FUV-bright young solar analog EK Dra is used as the illuminating radiation field. In a terrestrial atmosphere illuminated by an older solar-type star, the much stronger NUV flux would serve to balance the possible enhancement of O_3 (the O_3 photolysis threshold is at $\lambda \sim 2500$ Å). However the weak NUV field of GJ 876 should not destroy significant amounts of O_3. We therefore suggest that the relatively strong FUV flux may increase the amount of atmospheric O_3 present relative to what is predicted by models of terrestrial HZ planets orbiting "inactive" M-dwarfs (Segura et al. 2005). This highlights the need for measured UV spectra of the host star when modeling the atmospheric properties of an exoplanet. The paucity of UV observations of low-mass exoplanetary host stars may bias our interpretation of potential biomarkers when direct spectroscopy of extrasolar terrestrial planets becomes feasible, possibly in the coming decade with the James Webb Space Telescope (Belu et al. 2011).

4.2. Fluorescent Emission from Hot H_2

The COS spectra of GJ 876 show surprisingly strong emission from fluorescent H_2, excited by Lyα photons. Jupiter's dayglow and auroral spectra are dominated by collisionally-excited and Lyβ-pumped H_2 (Feldman et al. 1993; Gustin et al. 2002). However, emission from hot H_2 pumped by Lyα photons was observed at the Shoemaker-Levy 9 impact site (Wolven et al. 1997). If there were a heat source capable of producing high molecular temperatures ($T(H_2) > 2000$ K) in the atmosphere of GJ 876b or GJ 876c, then the ob-

served fluorescence could have an exoplanetary, rather than a stellar origin. Similar emission was searched for from the well-studied transiting planet HD 209458b, but not conclusively detected (France et al. 2010b).

We cannot rule out the possibility that some of the H_2 emission is associated with GJ 876b or GJ 876c, but a calculation of the available energy budget argues for a stellar origin for this fluorescence. From the reconstructed $Ly\alpha$ profile (§3.2), we can calculate the $Ly\alpha$ surface flux, $F_{surf}(Ly\alpha) = F_{obs}(Ly\alpha) \times (d/R_*)^2$, where R_* is the stellar radius $R_* \approx 0.3$ $R_\odot$. The $Ly\alpha$ flux absorbed by H_2 is then $F_{abs}(H_2) = F_{surf}(Ly\alpha) \times (1 - e^{-\tau_\lambda(H_2)})$, where $\tau_\lambda(H_2)$ is the optical depth of H_2, calculated for $N(H_2) = 10^{17}$ cm^{-2} (the absorbed flux increases by only a factor of ~ 2.5 when $N(H_2) = 10^{19}$ cm^{-2}) and $T(H_2) = 2500$ K. If we assume that the H_2 resides in an optically thin circular cloud, the emitted and absorbed luminosities will be equal, $L_{abs}(H_2) = \pi R_{H2}^2 F_{abs}(H_2) = L_{emis}(H_2)$. Focusing on the $[v',J'] = [1,4]$ progression, $L_{emis}(H_2) = 4\pi d^2 \times (F_{(1-7)P(5)}/B_{17})$, where $F_{(1-7)P(5)}$ is the flux in the H_2 $(1-7)P(5)$ $\lambda1504.76$ emission line ($F_{(1-7)P(5)} = (2.2 \pm 0.4) \times 10^{-16}$ erg cm^{-2} s^{-1}) and B_{17} is the $v' \rightarrow v'' = 1 \rightarrow 7$ branching ratio ($B_{17} = 0.115$). Equating $L_{emis}(H_2)$ and $L_{abs}(H_2)$, we find $R_{H2} = 0.32 \pm 0.13$ $R_\odot$, consistent with the H_2 being located in the stellar atmosphere. A similar calculation at the semi-major axis of GJ 876b would require $R_{H2} > 400 R_{Jup}$, much larger than observational or theoretical estimates of the size of hot Jupiter envelopes (Vidal-Madjar et al. 2008; Murray-Clay et al. 2009). We conclude that the observed fluorescence is produced by hot photospheric molecules illuminated by the strong chromospheric $Ly\alpha$ radiation field.

REFERENCES

Belu, A. R., Selsis, F., Morales, J.-C., Ribas, I., Cossou, C., & Rauer, H. 2011, A&A, 525, A83

Borucki, W. J., Koch, D. G., Basri, G., Batalha, N., Brown, T. M., Bryson, S. T., Caldwell, D., Christensen-Dalsgaard, J., Cochran, W. D., DeVore, E., Dunham, E. W., Gautier, III, T. N., Geary, J. C., Gilliland, R., Gould, A., Howell, S. B., Jenkins, J. M., Latham, D. W., Lissauer, J. J., Marcy, G. W., Rowe, J., Sasselov, D., Boss, A., Charbonneau, D., Ciardi, D., Doyle, L., Dupree, A. K., Ford, E. B., Fortney,

J., Holman, M. J., Seager, S., Steffen, J. H., Tarter, J., Welsh, W. F., Allen, C., Buchhave, L. A., Christiansen, J. L., Clarke, B. D., Das, S., Désert, J.-M., Endl, M., Fabrycky, D., Fressin, F., Haas, M., Horch, E., Howard, A., Isaacson, H., Kjeldsen, H., Kolodziejczak, J., Kulesa, C., Li, J., Lucas, P. W., Machalek, P., McCarthy, D., MacQueen, P., Meibom, S., Miquel, T., Prsa, A., Quinn, S. N., Quintana, E. V., Ragozzine, D., Sherry, W., Shporer, A., Tenenbaum, P., Torres, G., Twicken, J. D., Van Cleve, J., Walkowicz, L., Witteborn, F. C., & Still, M. 2011, ApJ, 736, 19

Correia, A. C. M., Couetdic, J., Laskar, J., Bonfils, X., Mayor, M., Bertaux, J.-L., Bouchy, F., Delfosse, X., Forveille, T., Lovis, C., Pepe, F., Perrier, C., Queloz, D., & Udry, S. 2010, A&A, 511, A21

Danforth, C. W., Keeney, B. A., Stocke, J. T., Shull, J. M., & Yao, Y. 2010, ApJ, 720, 976

Delfosse, X., Forveille, T., Perrier, C., & Mayor, M. 1998, A&A, 331, 581

Ehrenreich, D., Lecavelier Des Etangs, A., & Delfosse, X. 2011, A&A, 529, A80

Feldman, P. D., McGrath, M. A., Moos, H. W., Durrance, S. T., Strobel, D. F., & Davidsen, A. F. 1993, ApJ, 406, 279

France, K., Linsky, J. L., Brown, A., Froning, C. S., & Béland, S. 2010a, ApJ, 715, 596

France, K., Stocke, J. T., Yang, H., Linsky, J. L., Wolven, B. C., Froning, C. S., Green, J. C., & Osterman, S. N. 2010b, ApJ, 712, 1277

Gustin, J., Grodent, D., Gérard, J. C., & Clarke, J. T. 2002, Icarus, 157, 91

Hawley, S. L., Allred, J. C., Johns-Krull, C. M., Fisher, G. H., Abbett, W. P., Alekseev, I., Avgoloupis, S. I., Deustua, S. E., Gunn, A., Seiradakis, J. H., Sirk, M. M., & Valenti, J. A. 2003, ApJ, 597, 535

Hawley, S. L., Gizis, J. E., & Reid, I. N. 1996, AJ, 112, 2799

Herczeg, G. J., Wood, B. E., Linsky, J. L., Valenti, J. A., & Johns-Krull, C. M. 2004, ApJ, 607, 369

Joshi, M. 2003, Astrobiology, 3, 415

Kaltenegger, L., Segura, A., & Mohanty, S. 2011, ApJ, 733, 35

Kasting, J. F., Whitmire, D. P., & Reynolds, R. T. 1993, Icarus, 101, 108

Lee, A. Y. T., Yung, Y. L., Cheng, B.-M., Bahou, M., Chung, C.-Y., & Lee, Y.-P. 2001, ApJ, 551, L93

Linsky, J. L., Diplas, A., Wood, B. E., Brown, A., Ayres, T. R., & Savage, B. D. 1995, ApJ, 451, 335

Linsky, J. L., Draine, B. T., Moos, H. W., Jenkins, E. B., Wood, B. E., Oliveira, C., Blair, W. P., Friedman, S. D., Gry, C., Knauth, D., Kruk, J. W., Lacour, S., Lehner, N., Redfield, S., Shull, J. M., Sonneborn, G., & Williger, G. M. 2006, ApJ, 647, 1106

Linsky, J. L. & Wood, B. E. 1994, ApJ, 430, 342

Marcy, G. W., Butler, R. P., Fischer, D., Vogt, S. S., Lissauer, J. J., & Rivera, E. J. 2001, ApJ, 556, 296

Marcy, G. W., Butler, R. P., Vogt, S. S., Fischer, D., & Lissauer, J. J. 1998, ApJ, 505, L147

Mota, R., Parafita, R., Giuliani, A., Hubin-Franskin, M., Lourenco, J. M. C., Garcia, G., Hoffmann, S. V., Mason, N. J., Ribeiro, P. A., Raposo, M., & Limao-Vieira, P. 2005, Chemical Physics Letters, 416, 152

Murray-Clay, R. A., Chiang, E. I., & Murray, N. 2009, ApJ, 693, 23

Osten, R. A., Hawley, S. L., Allred, J. C., Johns-Krull, C. M., & Roark, C. 2005, ApJ, 621, 398

Osterman, S., Green, J., Froning, C., Béland, S., Burgh, E., France, K., Penton, S., Delker, T., Ebbets, D., Sahnow, D., Bacinski, J., Kimble, R., Andrews, J., Wilkinson, E., McPhate, J., Siegmund, O., Ake, T., Aloisi, A., Biagetti, C., Diaz, R., Dixon, W., Friedman, S., Ghavamian, P., Goudfrooij, P., Hartig, G., Keyes, C., Lennon, D., Massa, D., Niemi, S., Oliveira, C., Osten, R., Proffitt, C., Smith, T., & Soderblom, D. 2011, Ap&SS, 157

Pagano, I., Linsky, J. L., Carkner, L., Robinson, R. D., Woodgate, B., & Timothy, G. 2000, ApJ, 532, 497

Poppenhaeger, K., Robrade, J., & Schmitt, J. H. M. M. 2010, A&A, 515, A98+

Redfield, S. & Linsky, J. L. 2008, ApJ, 673, 283

Rivera, E. J., Laughlin, G., Butler, R. P., Vogt, S. S., Haghighipour, N., & Meschiari, S. 2010, ApJ, 719, 890

Rivera, E. J., Lissauer, J. J., Butler, R. P., Marcy, G. W., Vogt, S. S., Fischer, D. A., Brown, T. M., Laughlin, G., & Henry, G. W. 2005, ApJ, 634, 625

Segura, A., Kasting, J. F., Meadows, V., Cohen, M., Scalo, J., Crisp, D., Butler, R. A. H., & Tinetti, G. 2005, Astrobiology, 5, 706

Segura, A., Krelove, K., Kasting, J. F., Sommerlatt, D., Meadows, V., Crisp, D., Cohen, M., & Mlawer, E. 2003, Astrobiology, 3, 689

Segura, A., Meadows, V. S., Kasting, J. F., Crisp, D., & Cohen, M. 2007, A&A, 472, 665

Segura, A., Walkowicz, L. M., Meadows, V., Kasting, J., & Hawley, S. 2010, Astrobiology, 10, 751

Shankland, P. D., Blank, D. L., Boboltz, D. A., Lazio, T. J. W., & White, G. 2008, AJ, 135, 2194

Udry, S., Bonfils, X., Delfosse, X., Forveille, T., Mayor, M., Perrier, C., Bouchy, F., Lovis, C., Pepe, F., Queloz, D., & Bertaux, J.-L. 2007, A&A, 469, L43

Vidal-Madjar, A., Lecavelier des Etangs, A., Désert, J.-M., Ballester, G. E., Ferlet, R., Hébrard, G., & Mayor, M. 2008, ApJ, 676, L57

Walkowicz, L. M., Johns-Krull, C. M., & Hawley, S. L. 2008, ApJ, 677, 593

Welsh, B. Y., Wheatley, J. M., Seibert, M., Browne, S. E., West, A. A., Siegmund, O. H. W., Barlow, T. A., Forster, K., Friedman, P. G., Martin, D. C., Morrissey, P., Small, T., Wyder, T., Schiminovich, D., Neff, S., & Rich, R. M. 2007, ApJS, 173, 673

West, A. A., Hawley, S. L., Walkowicz, L. M., Covey, K. R., Silvestri, N. M., Raymond, S. N., Harris, H. C., Munn, J. A., McGehee, P. M., Ivezić, Ž., & Brinkmann, J. 2004, AJ, 128, 426

Wolven, B. C., Feldman, P. D., Strobel, D. F., & McGrath, M. A. 1997, ApJ, 475, 835

Wood, B. E., Linsky, J. L., & Ayres, T. R. 1997, ApJ, 478, 745

Wood, B. E., Redfield, S., Linsky, J. L., Müller, H.-R., & Zank, G. P. 2005, ApJS, 159, 118

Woods, T. N., Chamberlin, P. C., Harder, J. W., Hock, R. A., Snow, M., Eparvier, F. G., Fontenla, J., McClintock, W. E., & Richard, E. C. 2009, Geophys. Res. Lett., 36, 1101

Wordsworth, R. D., Forget, F., Selsis, F., Madeleine, J.-B., Millour, E., & Eymet, V. 2010, A&A, 522, A22+

Yoshino, K., Esmond, J. R., Sun, Y., Parkinson, W. H., Ito, K., & Matsui, T. 1996, J. Quant. Spec. Radiat. Transf., 55, 53
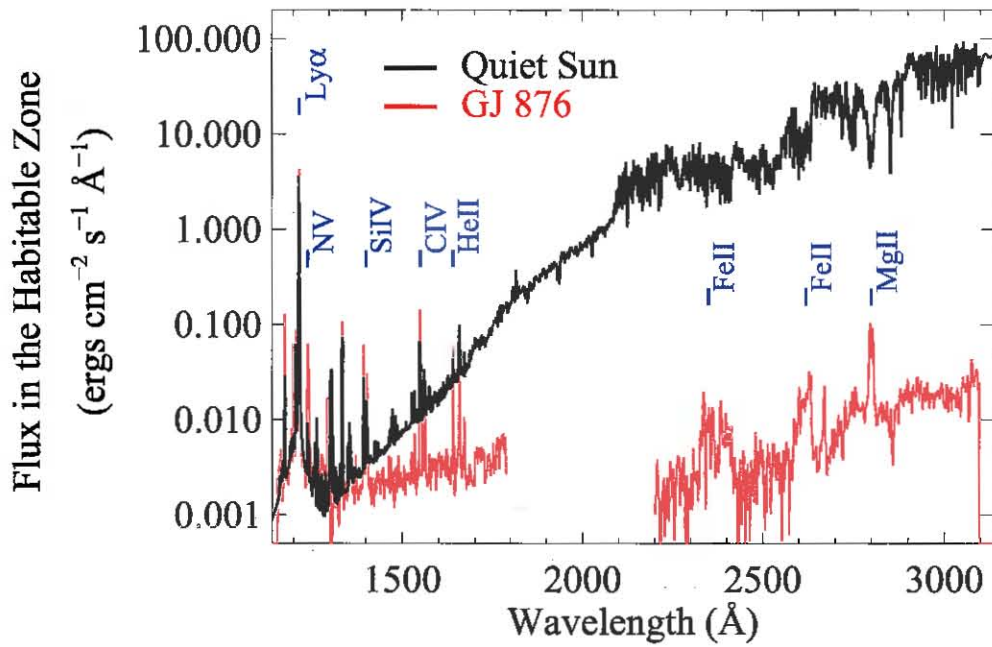
Fig. 1.— A comparison of the solar 1150 – 3140 Å flux incident on the habitable zone of the Solar System (solar flux at 1 AU, *black*) and the observed flux from GJ 876 in the HZ (at 0.21 AU, *red*). The 1800 – 2200 Å region for GJ 876 has been excluded due to low S/N.
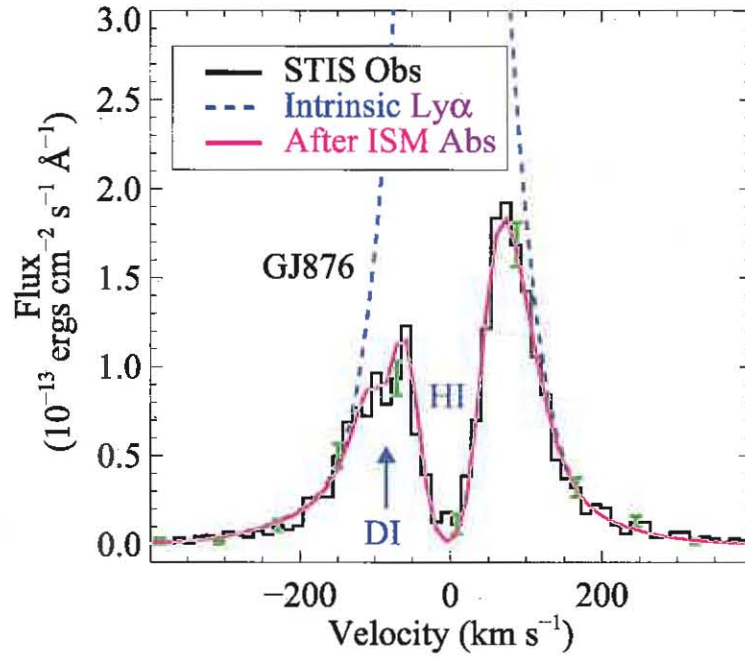
Fig. 2.— Velocity profile of the stellar Lyα emission line. The STIS G140M observation of GJ876 is displayed as the black histogram, with representative error bars plotted in green. The Lyα line profile was reconstructed by assuming a 2-component Gaussian emission line (*blue dashed line*) and correcting for interstellar neutral hydrogen and deuterium ($N(\mathrm{HI}) = 1.1 \times 10^{18}$ cm^{-2}, $b = 8.0$ km s^{-1}, D/H $= 1.5 \times 10^{-5}$; the final model is shown in *magenta*). Interstellar hydrogen and deuterium absorption lines are marked.

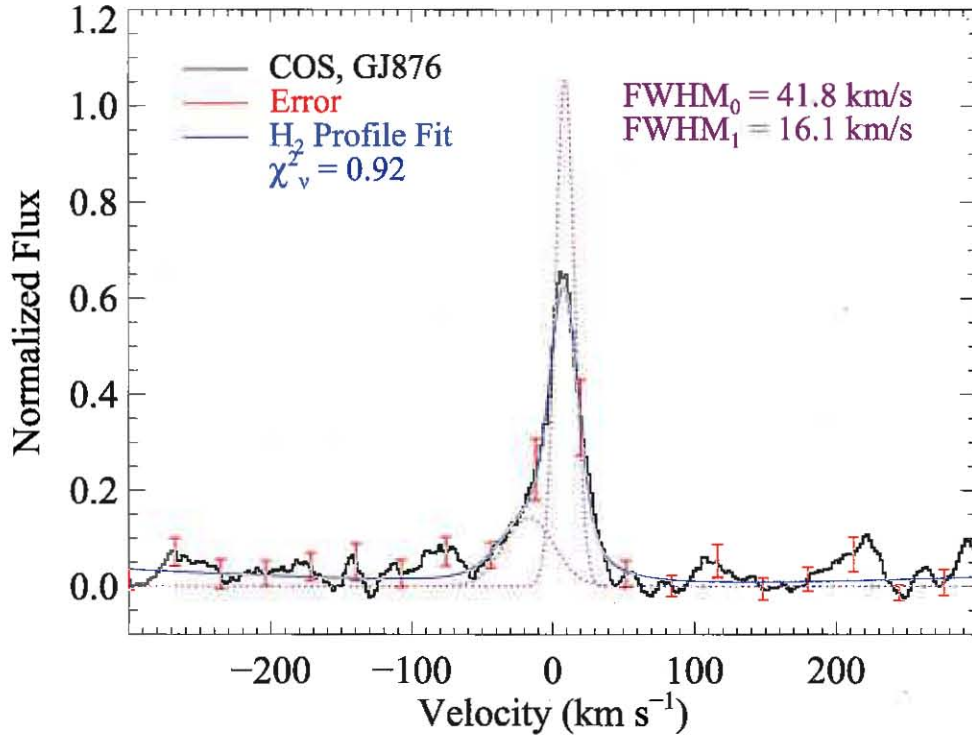Fig. 3.— Co-added velocity profile of six fluorescent H_2 emission lines observed by COS. The narrow emission component is unresolved (FWHM$_{H2}$ = 16.1 km s^{-1}) and consistent with the stellar radial velocity of +8.7 km s^{-1} (v_{H2} = 9.0 km s^{-1}). The weaker, broad component (offset by -26 km s^{-1}) is only marginally detected. The dotted lines are the intrinsic Gaussian H_2 emission lines and the overplotted solid blue line is the H_2 spectral fit convolved with the COS LSF.
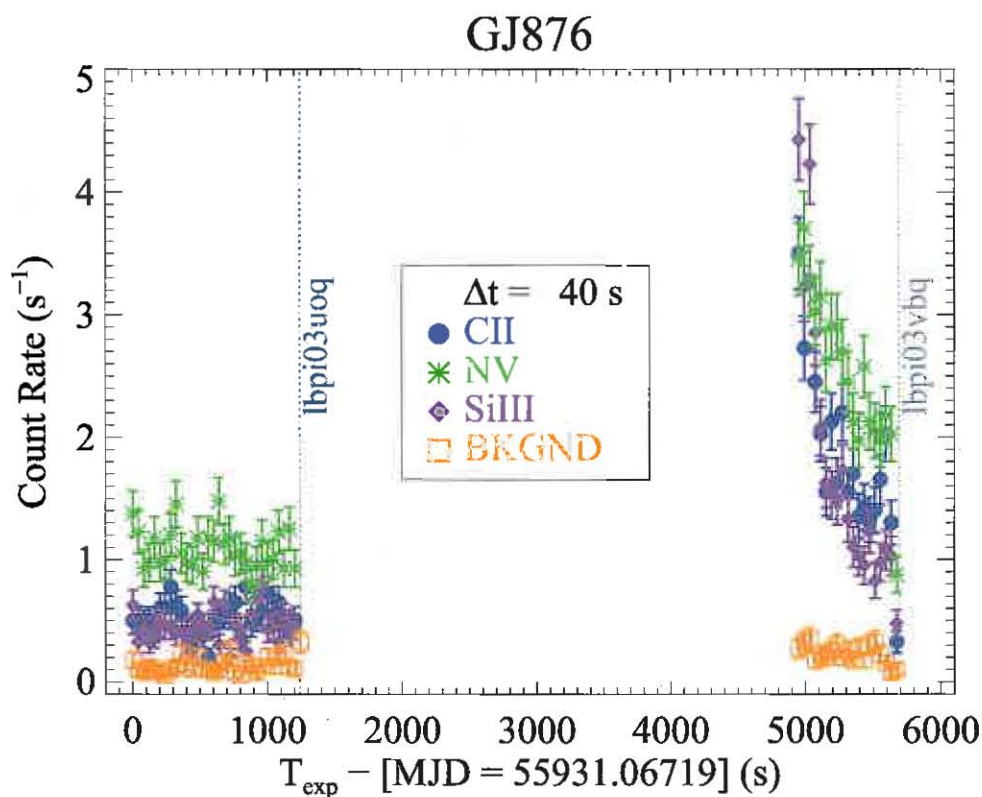
Fig. 4.— Direct observation of an FUV flare on the so-called "inactive" M-dwarf GJ 876 with *HST*-COS. The count rates in various chromospheric and transition region emission lines – C II $\lambda 1335$Å[*blue circles*], N V $\lambda 1240$Å[*green stars*], Si III $\lambda 1206$Å[*purple diamonds*] – are displayed versus the time of observation. The peak observed flare emission is $\approx 10\times$ the quiescent level, although the true flare peak (which apparently occurred during Earth occultation) could have been much larger. The COS data were binned to 40 s intervals for this plot. The detector background level is shown as orange squares.

Table 1. Habitable Zone UV Fluxes.

	$\Delta\lambda^a$ (Å)	Solar[b] (ergs cm^{-2} s^{-1})	GJ876[c] (ergs cm^{-2} s^{-1})
$F(\mathrm{Ly}\alpha)^d$	(1210 – 1220)	5.6×10^0	$9.5\ (\pm 0.7) \times 10^0$
$F(\mathrm{N\ V})$	(1235 – 1245)	1.8×10^{-2}	$2.0\ (\pm 0.1) \times 10^{-1}$
$F(\mathrm{Si\ IV})$	(1390 – 1410)	5.6×10^{-2}	$1.9\ (\pm 0.1) \times 10^{-1}$
$F(\mathrm{C\ IV})$	(1545 – 1555)	1.2×10^{-1}	$4.2\ (\pm 0.3) \times 10^{-1}$
$F(\mathrm{He\ II})$	(1635 – 1645)	2.4×10^{-2}	$1.2\ (\pm 0.1) \times 10^{-1}$
$F(\mathrm{FUV})$	(1150 – 1210) + (1220 – 1790)	1.8×10^1	$4.1\ (\pm 0.6) \times 10^0$
$F(\mathrm{NUV})$	(2200 – 3140)	2.2×10^4	$9.8\ (\pm 0.6) \times 10^0$
$F(\mathrm{Ly}\alpha)/F(\mathrm{FUV})$		0.3	2.3
$F(\mathrm{Ly}\alpha)/F(\mathrm{FUV+NUV})$		2.6×10^{-4}	0.7

[a]$\Delta\lambda$ is the bandpass over which the flux is calculated.

[b]Observed Solar flux at 1 AU.

[c]Observed UV Flux scaled to the orbit of GJ 876b, $F_{HZ} = F_{obs} \times (4.7\ \mathrm{pc}\ /\ 0.21\ \mathrm{AU})^2$.

[d]Intrinsic Lyα flux after correction for interstellar absorption.